Effect of Oxygen Concentration on the Oxidative Thermodynamics and Spontaneous Combustion of Pulverized Coal

Lifeng Ren,* Qingwei Li,* Jun Deng, Li Ma, Yang Xiao, Xiaowei Zhai, and Jianchi Hao

ABSTRACT: Spontaneous combustion of pulverized coal has become a safety topic and has been extensively researched. This study using differential scanning calorimetry investigated the exothermic characteristics and spontaneous combustion risk of three metamorphic pulverized coal samples during oxidative combustion, for oxygen concentrations of 21, 19, 17, 15, 13, 11, 9, 7, and 5 vol %. Results indicated that decreased oxygen concentrations reduced exothermic intensity and substantially increased ignition temperatures. The oxidative thermal release observed during the combustion stage was conspicuously higher than during the low-temperature oxidation stage. Thermal release during low-temperature oxidation was low during low oxygen concentrations; however, when the oxygen concentration was less than 13.0 vol.%, it had a considerable influence on exothermic combustion. When the oxygen level was lowered from 21.0 to 5.0 vol %, spontaneous combustion risk indexes lessened from 2.07 (sample A), 1.85 (sample B), and 0.81 [J/(mg min °C²)] (sample C) to 1.08 (sample A), 1.13 (sample B), and 0.40 [J/(mg min °C²)] (sample C), respectively. Both apparent activation energy and spontaneous combustion risk indexes of the samples decreased saliently as oxygen concentration decreased. Thus, reducing oxygen concentration would be an effective method of inhibiting or possibly even preventing the spontaneous combustion of pulverized coal.
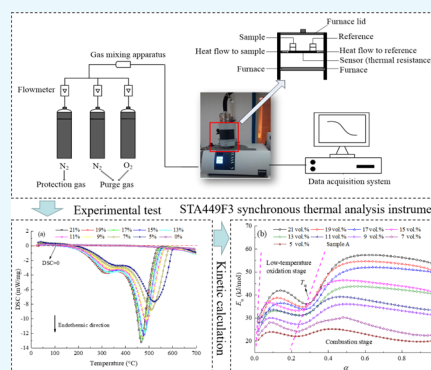
1. INTRODUCTION

Coal is a kind of fuel and industrial materials, which is distributed extensively on the earth.[1,2] It is widely used in the fields of power generation,[3] chemical industries,[4] and heating because of its low cost and easy exploitation.[5] Lump coal usually is pulverized into powder to improve the combustion and chemical conversion efficacy.[6−8] Moreover, pulverization is considered that noticeably reduces the emission of pollutants when combustion occurs.[9] However, pulverized coal provides strong chemical reactivity and large surface area, which may undergo spontaneous combustion during production, transportation, storage, and even disposal.[10,11] Spontaneous combustion of pulverized coal seriously threatens safety of the producers and industry infrastructure. Numerous publications have investigated the characteristics of coal spontaneous combustion[12,13] and approach to enhance the combustion efficiency and reduce the emissions from pulverized coal.[14] The oxidative combustion properties of pulverized coal are the key factors affecting its combustion efficiency and emission amounts. Therefore, plenty of experimental techniques have been adopted to examine coal oxidation and combustion, including thermogravimetry,[5,15] thermal release,[16] and combustion reaction,[17] which have provided more detailed insights into the oxidative combustion properties of pulverized coal under a variety of oxygen-enriched atmospheres and with different particle sizes.

Particle size is a vital factor affecting the oxidative combustion peculiarities of pulverized coal. For example, with the particle size diminution, the ignition temperature decreased; meanwhile, the burn rate increased.[18,19] Moreover, when the superficial area and hole volume were increased, both thermal release and combustion were increased.[20,21] There exist a critical value for the particle size of pulverized coal between emission concentration of pollutants such as NO_x and particle size. When particle size was smaller than the critical value, the emission concentration of pollutants such as NO_x reduced along with reduction in the particle size. For instance, the NO_x reduction efficiency of superfine pulverized coal is superior to that of regular size.[22,23] Notably, the production of pulverized coal involves mechanical pulverization and drying at a high temperature, as well as increasing the surface area, types, and amounts of active structures.

Pulverized coal is mostly produced and stored in semi-enclosed spaces. The oxidation of pulverized coal consumes

oxygen, which is responsible for most incidences of spontaneous combustion at oxygen concentrations below 21.0 vol %. Oxygen concentration substantially affects the combustion characteristics of pulverized coal,[24] and decreasing oxygen concentration can inhibit low-temperature exothermic oxidation.[25] A considerable lag phenomenon was discovered in thermal flux curves as oxygen concentration decreased.[26] The critical temperature of coal was influenced by oxygen concentration, heating rate, and particle size.[27] The oxygen concentration affected the release rates of CO and CO_2. The release rate of CO is higher than that of CO_2 at 21.0 vol. % oxygen; however, the rate of release of CO_2 was higher than that of CO at 15.0 vol. % oxygen.[28] The value of thermokinetic parameters increased with a decrease in the oxygen concentration during low-temperature oxidation of coal.[29] The oxygen consumption rate of coal decreased with the decrease in the oxygen level.[30] Oxygen-depleted circumstances inhibited the oxidation of the reactive structure of coal;[31] therefore, the technology that reduced the oxygen concentration in the local environment was a control method for spontaneous combustion in goaf of mine, coal bunker, and coalfield fire.[32] Pulverized coal can readily adsorb an immerse amount of oxygen, which means that the spontaneous combustion characteristics were different from those of unpulverized coal under the same conditions. As yet, few studies had been conducted in the oxidative thermal release characteristics of pulverized coal at low oxygen levels. Moreover, few scientific evaluations had been conducted on the spontaneous combustion hazards and oxidative thermokinetics of pulverized coal in oxygen-lean circumstances. This lack of investigation of pulverized coal had limited the evaluation of spontaneous combustion hazards and prevented the development of more detailed thermal hazard models.

To delve into the exothermic properties and evaluate the risks of spontaneous combustion of pulverized coal at various oxygen concentrations, this study explored the oxidative thermodynamics and self-ignition of pulverized coal at diverse oxygen-level atmospheres. The research objectives were to (1) investigate the non-linear characteristics of oxidation exotherm for the pulverized coal, (2) explore the changes in thermodynamic parameters during oxidation combustion of pulverized coal under various oxygen levels and temperatures, and (3) evaluate the risks of spontaneous combustion of pulverized coal under different oxygen concentrations. Results indicated that reducing oxygen concentrations inhibited spontaneous combustion. The risk of spontaneous combustion of pulverized coal under different oxygen concentration conditions is evaluated, and guidance is provided for reducing the oxygen concentration for the environment inert to prevent and control spontaneous combustion during the production and transportation of pulverized coal. However, it can be used as a basis for further developing prevention and control schemata for pulverized coal spontaneous combustion occurrence.

2. EXPERIMENTAL AND METHODS

2.1. Samples. In thermal power and chemical industry applications, bituminous coal is primarily used in the form of pulverized coal. Therefore, three different metamorphic bituminous pulverized coal samples were gleaned from three separate sources in China, (i) cannel coal (low-metamorphic, sample A); (ii) gas-fat (coal medium-metamorphic, sample B); and (iii) meagre coal (high-metamorphic, sample C). These pulverized coal samples were all of the bituminous and were obtained directly from the localized and pulverized coal production systems. The particle size range of the pulverized coal sample is less than 70 μm, and the D50 particle size is shown in Table 1. The pulverized coal samples were

Table 1. Proximate Analysis and Average Particle Sizes of the Three Pulverized Coal Samples

| sample | proximate analysis (mass %) | | | | D50 particle size (μm) |
	moisture	ash	volatile	fixed carbon	
sample A	5.21	8.96	31.03	54.80	27.0
sample B	2.06	8.75	32.28	56.91	26.0
sample C	0.92	10.8	16.22	72.06	34.0

encapsulated in plastic bags, placed in glass-stoppered bottles, and transported to the laboratory for further analysis. The properties of the three selected coals were tested by 5E-MAG6700 Automatic Proximate Analysis (air dry base). The proximate analysis of samples is presented in Table 1.

2.2. Experimental Systems and Conditions. The differential scanning calorimetry (DSC) installation was applied to measure the oxidative exothermic process of samples during oxidative combustion (Figure 1). The mass of the measured sample was approximately 10 mg, which was placed in the ceramic reaction cell. During the DSC experiments, different nitrogen−oxygen mixtures with 21.0, 19.0, 17.0, 15.0, 13.0, 11.0, 9.0, 7.0, and 5.0 vol. % oxygen were introduced into the chamber. The samples in the reaction cell contacted with the atmosphere in the chamber under open conditions, whereas the gases diffused inward through the pores in coal and voids between the particles. The supplied volume of gas, 100 mL/min, was constant. The ramp rates of the DSC experiment under each oxygen concentration were 2.5, 5.0, 10.0, and 15.0 °C/min. Then, the samples were heated from 30 to 800 °C.

2.3. Analytical Methods. *2.3.1. Calculation Method for Determination of Apparent Activation Energy.* The oxidative exothermic process of pulverized coal follows the first type of thermokinetic equation.[27] Equation 1 is obtained from Arrhenius method

$$\frac{d\alpha}{dT} = \frac{A}{\beta}\exp\left(-\frac{E_\alpha}{RT}\right)f(\alpha) \tag{1}$$

where α is the conversion degree, β is the heating rate (°C/min), A is the pre-exponential factor (1/s), T is the temperature (°C), E_α is the apparent activation energy (kJ/mol), and R is the universal gas constant.

To explore the apparent activation energy (E_α) during oxidative combustion of coal, non-isothermal and multi-heating rate methods were used. However, multi-heating rate methods, such as the Kissinger−Akahira−Sunose (KAS) and Flynn−Wall−Ozawa (FWO) methods, avoid errors possibly caused by the selection of the proper mechanism function. The FWO and KAS methods are represented by eqs 2 and 3, respectively[33]

$$\log(\beta_i) = \text{const} - 1.052\frac{E_\alpha}{RT_\alpha} \tag{2}$$
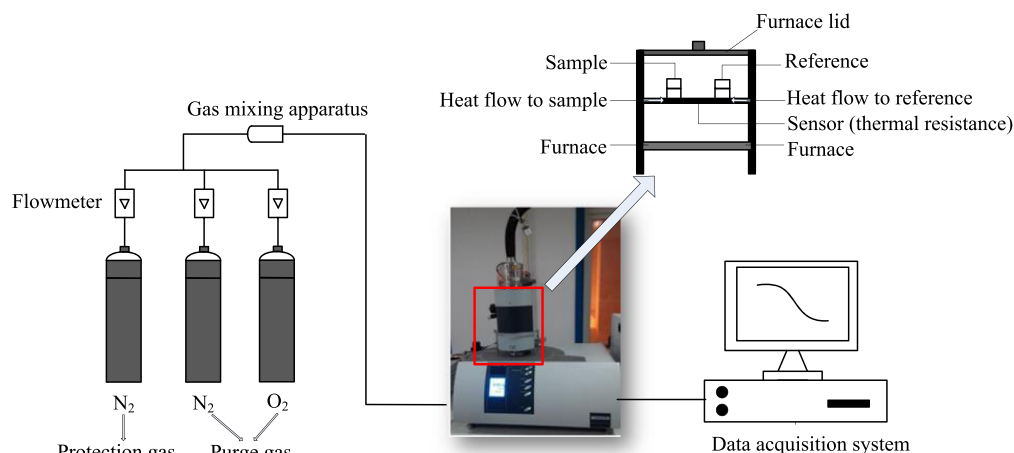
Figure 1. STA449F3 synchronous thermal analysis instrument.

$$\log\left(\frac{\beta_i}{T_{\alpha,i}{}^2}\right) = \text{const} - \frac{E_\alpha}{RT_\alpha} \tag{3}$$

where β is the heating rate (°C/min), i is the constant in different heating rate experiments, T_α is the temperature at conversion degree α (°C), and $T_{\alpha,i}$ is the temperature at conversion degree α and i experiment (°C).

In essence, the Starink method provides a more accurate apparent activation energy value than other model-free methods, such as the FWO, Kissinger, and Boswell methods. The Starink method is presented in eq 4[33]

$$\log\left(\frac{\beta_i}{T_{\alpha,i}{}^{1.92}}\right) = \text{const} - 1.0008\frac{E_\alpha}{RT_\alpha} \tag{4}$$

2.3.2. Evaluation Method for Spontaneous Combustion Risk. The spontaneous combustion risk of coal denotes the capability of coal–oxygen reactions from ambient temperature to ignition. Therefore, the lower the ignition temperature, the shorter the period reaching to the ignition temperature, or the more heat release in the oxidation stage will result in an easier occurrence for spontaneous combustion of coal. A comprehensive index (ε) was used to estimate the risks of spontaneous combustion of the pulverized coal sample (eq 5).[34] The higher the value of ε, the higher the risks of spontaneous combustion of the pulverized coal sample, as indicated by eq 5

$$\varepsilon = \frac{Q_{ig}}{(t_{ig} - t_{exo})T_{ig}T_{exo}} = \frac{\beta\int_{t_{exo}}^{t_{ig}} q(t)\mathrm{d}t}{T_{ig}T_{exo}(T_{ig} - T_{exo})} \tag{5}$$

where ε is the index of spontaneous combustion risk [J/(mg min °C^2)], Q_{ig} is the thermal release in the low-temperature oxidation stage (J/g), $q(t)$ is the thermal release rate at t (J/g), T_{ig} is the ignition temperature (°C), T_{exo} is the starting temperature of thermal release (°C), t_{exo} is the time to reach T_{exo} (s), and t_{ig} is the time to reach T_{ig} (s).

3. RESULTS AND DISCUSSION

3.1. Exothermic Characteristic of the Pulverized Coal Sample. The DSC and the differential coefficient of the DSC (DDSC) curves of the samples at a ramp rate of 5 °C/min and various oxygen concentrations are illustrated in Figure 2.

3.1.1. Variation in DSC and DDSC Curves with Temperature. The DSC and DDSC curves under different oxygen concentrations presented a similar trend with the increase in temperature. There are two intersection points between the DDSC curve and the coordinate axis (DDSC value is 0), which indicated that the DSC curve was a typical double-exothermic peak curve.[35−37] The two intersection points correspond to the peak temperature of the two exothermic peaks of the DSC curve. Although the bimodal characteristics of the DSC curve under low oxygen concentrations were not obvious, it exists in fact. Taking the DSC curve under 21 vol. % oxygen concentration as an example, the corresponding temperature of the first (earlier) peak was approximately 300 °C. The corresponding temperature of the second (later) peak for samples A and B was approximately 470 °C (Figure 2). However, the corresponding temperature of the second peak of sample C was approximately 500 °C. When the temperature exceeded 200 °C, the DDSC curves exhibited two distinct peaks above and below a DDSC value of 0 (Figure 2). This phenomenon was caused by the difference in the categories and amounts of active functional groups in the pulverized coal. During the oxidative combustion of pulverized coal, active structures were continuously activated and participated throughout the oxidation reaction. However, it was different in the activity for different functional groups. Some active structures (e.g., alkyl chains, methyl groups, and carboxyl groups) were readily oxidized during the low-temperature stage, and the first peak on the DSC resulted from the concentrated reaction of these high-activity functional groups. However, other stable structures (e.g., aromatic structures) required considerably higher energy and temperature levels for activation,[38] then the second peak was formed. Among the three pulverized coal samples, sample A had the lowest degree of deterioration, and the content of alkyl chains, methyl groups, and carboxyl groups was higher, resulting in sample A exhibiting higher oxidation reaction activity and lower peak temperature of the exothermic peak. However, sample C had the highest degree of deterioration, with lower alkyl chain, methyl, and carboxyl contents, and more stable structure with higher aromatic structure content. As a result, sample C exhibited lower oxidation reactivity, and the peak temperature of the exothermic peak increased significantly.

3.1.2. Effects of Oxygen Levels on the Exothermic Characteristic. The DSC and DDSC curves of the same
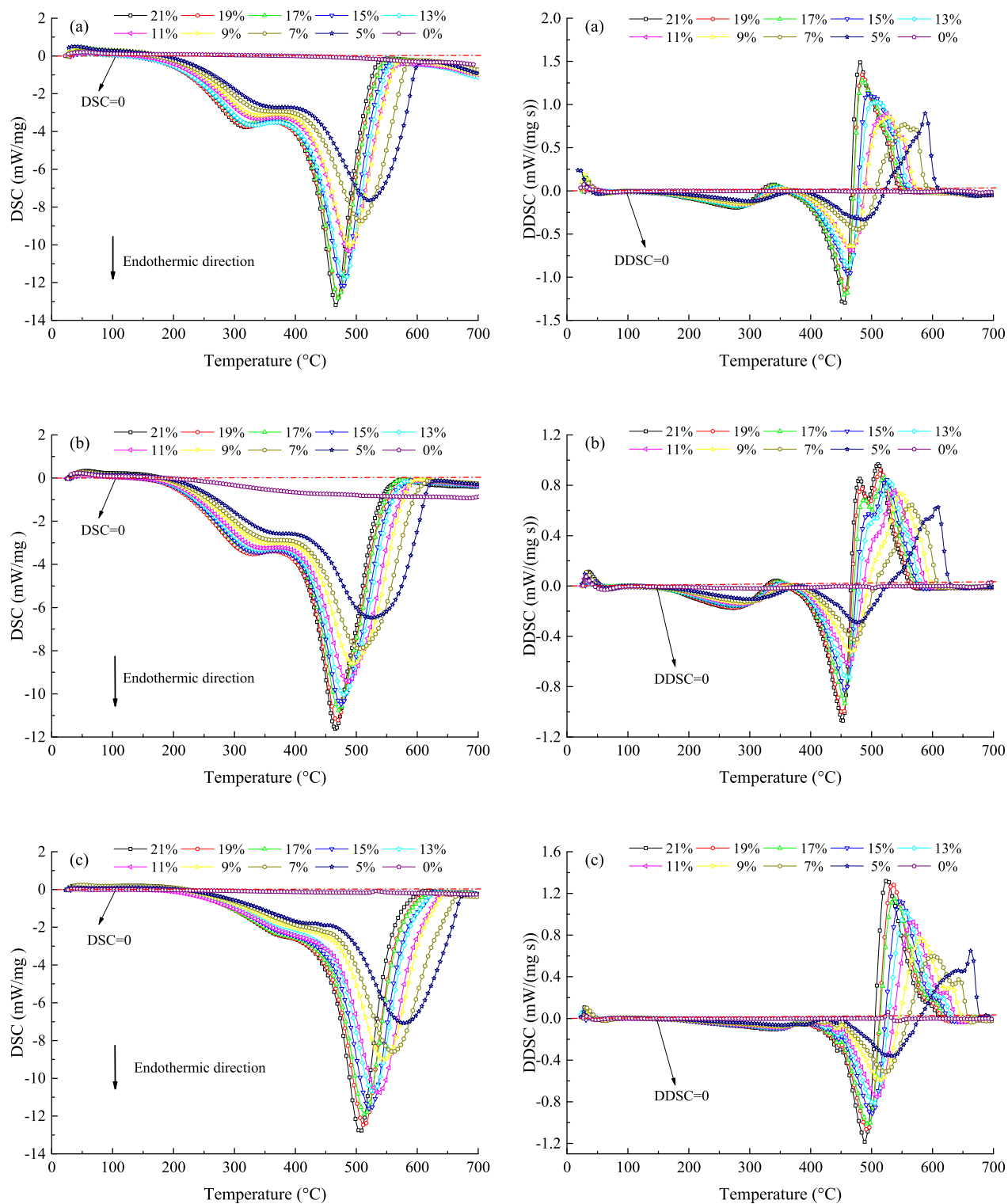
Figure 2. DSC and DDSC curves during the oxidative combustion of the test sample with various oxygen levels at a heating rate of 5.0 °C/min: (a) sample A, (b) sample B, and (c) sample C.

pulverized coal were similar for various oxygen levels (5.0–21.0 vol. %; Figure 2). When the nitrogen concentration was 100.0 vol. %, the DSC curves were close to 0 mW/mg and only the DSC curve of the sample B exhibited an increase. The DSC values at 100.0 vol. % nitrogen were remarkably inferior to those at other oxygen concentration conditions. It meant that enough oxygen was a key factor affecting the thermal release

characteristics of sample oxidation. As the oxygen concentration reduced, the DSC and DDSC curves of samples showed an obvious lagged phenomenon, and the values along the curves were notably lower.

The aforementioned results were accredited to two factors: (1) A reduction in the oxygen concentration resulted in a decrease in the amount of activated oxygen molecules, which
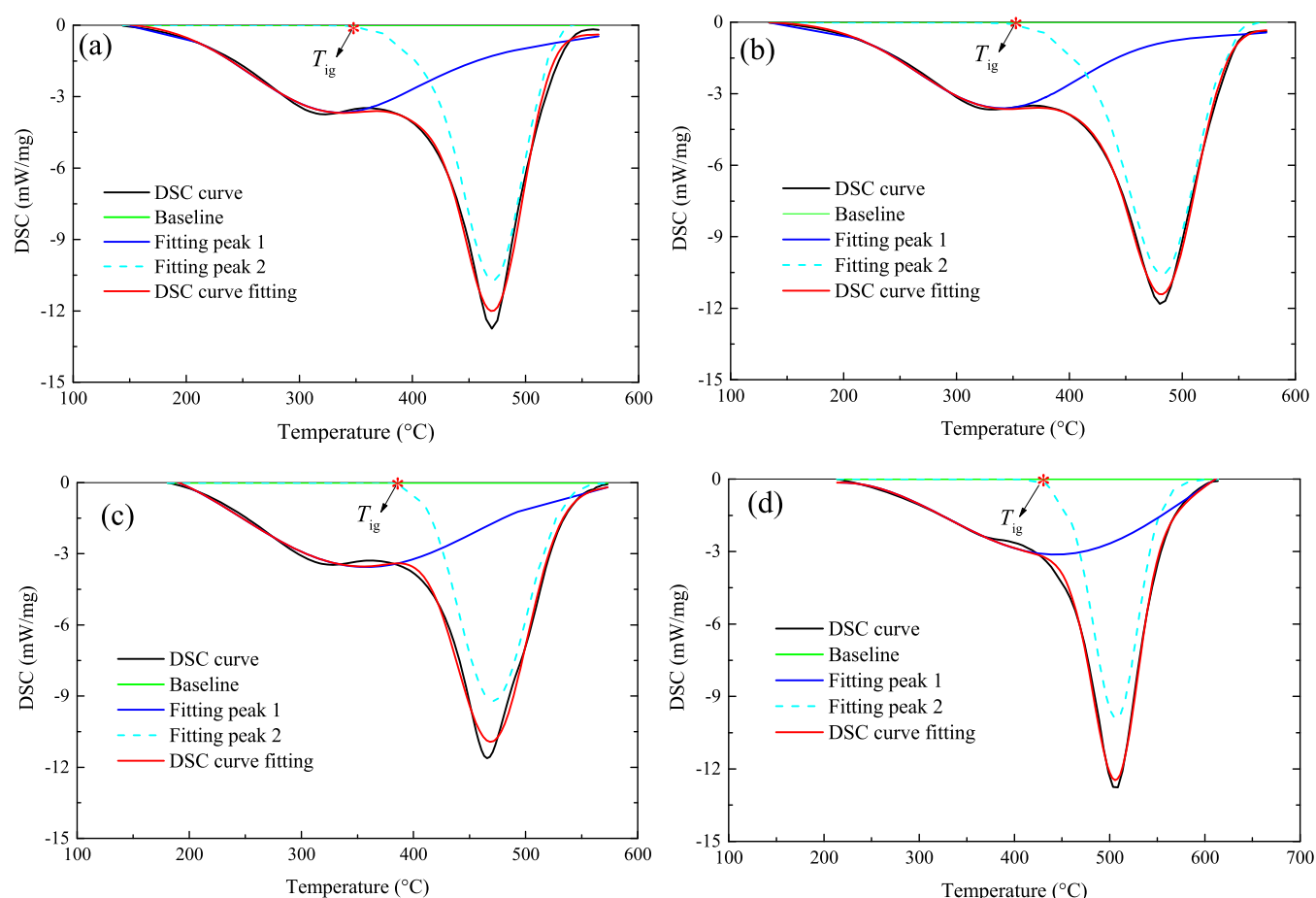
Figure 3. Results of the exothermic peak fitting during the oxidative combustion of pulverized coal at a heating rate of 5.0 °C/min: (a) sample A at an oxygen level of 21.0 vol. %, (b) sample A at an oxygen level of 13.0 vol. %, (c) sample B at an oxygen level of 21.0 vol. %, and (d) sample C at an oxygen level of 21.0 vol. %.

Table 2. Fitting Parameters of the DSC Curve of Sample A under Different Oxygen Concentrations

oxygen concentration (vol. %)	fitting peak	v_0	T_c	S	w	a_3	a_4	R^2
21	1	−0.02	364.05	−774.01	89.23	0.79	−0.046	0.995
	2		461.36	−765.79	30.16	−0.81	−0.088	
19	1	−0.02	364.05	−775.52	89.32	0.78	−0.049	0.994
	2		461.38	−764.82	30.13	−0.81	−0.088	
17	1	−0.01	324.81	−897.54	95.34	−0.63	−0.752	0.993
	2		470.19	−674.90	26.32	−0.19	0.030	
15	1	−0.01	375.54	−725.93	90.39	1.05	0.114	0.996
	2		469.50	−804.79	31.65	−0.70	−0.043	
13	1	−0.02	379.14	−679.69	88.99	1.30	0.217	0.998
	2		473.01	−845.99	33.38	−0.64	−0.015	
11	1	−0.07	387.17	−555.29	87.54	1.73	0.402	0.999
	2		481.15	−826.34	35.58	−0.53	0.060	
9	1	−0.03	339.86	−606.75	74.85	−0.31	−0.346	0.998
	2		490.02	−767.84	33.94	−0.13	0.168	
7	1	−0.01	365.33	−795.98	103.45	−0.32	−0.501	0.996
	2		504.99	−653.98	36.18	−0.40	0.061	
5	1	−0.02	373.01	−571.34	82.94	0.04	−0.204	0.998
	2		565.24	−424.90	46.74	2.90	2.744	

inhibited the chemical reaction between the oxygen and the active structures of the pulverized coal.[24] (2) When the oxygen concentration in the environment decreased, the oxygen gradient from the surface to the interior pores of the pulverized coal also decreased.[3] Low oxygen gradient suppressed the

diffusion of oxygen into the interior pores of the pulverized coal, inhibiting further oxidation of active structures. Under these influences, the active functional groups tend to be consumed step-by-step, resulting in hysteresis for the reaction of certain functional groups. The exothermic rate at the same

Table 3. Ignition Temperature of the Oxidation Stage of the Samples at a Heating Rate of 5.0 °C/min

sample	oxygen level (vol. %)								
	21	19	17	15	13	11	9	7	5
sample A	345.1	345.6	346.1	347.6	349.3	355.4	365.5	378.9	398.3
sample B	358.6	359.1	360.5	361.7	363.8	365.9	372.1	383.4	393.4
sample C	375.8	376.7	378.2	383.1	389.8	396.5	406.6	418.3	436.2

stage decreased. Therefore, the DSC and DDSC curves under lower oxygen concentrations lagged behind these under higher oxygen concentrations. Moreover, the incomplete oxidation reaction occupied a larger proportion when the oxygen concentration decreased.[25] Exothermic data from the incomplete oxidation reaction were markedly lower than that of the complete oxidation reaction, which exacerbated the decrease in the exothermic rate. This meant that the oxidative exothermic ability of pulverized coal can be considerably suppressed by lessening the local oxygen concentration.

3.2. Determination of Ignition Temperatures from the DSC Curves. *3.2.1. Ignition Temperature.* The DSC curves were typical bimodal curves of pulverized coal.[35] The bimodal characteristics of the DSC curves were investigated using the mathematical peak fitting method. Comparison analysis indicated that the Gram−Charlier A series (GCAS) peak function was suitable for peak fitting. The GCAS equation is given in eq 6. Figure 3 shows the peak fitted results for at a ramp rate of 5 °C/min under various oxygen concentrations. The fitting parameters of the DSC curve for the sample A under different atmospheres are presented in Table 2.

$$v = v_0 + \frac{S}{w\sqrt{2\pi}} e^{-z^2/2} \left(1 + \sum_{i=3}^{4} \frac{a_i}{i!} H_i(z)\right) \tag{6}$$

where v and a_i are fitting parameters of the DSC curve; z is an independent variable; $z = (T - T_c)/w$, $H_i(z)$ is the function of z; $H_3 = z^3 - 3z$, $H_4 = z^4 - 6z^3 + 3$; v_0 is the baseline of peak fit DSC curve (mW/mg); w is half-peak breadth of the DSC fit curve (°C); S is the area of the peak fit DSC curve; and T_c is the center temperature of the peak fit DSC curve (°C).

The DSC curve can be fitted to two exothermic peaks: the first exothermic peak (peak 1) and second exothermic peak (peak 2) can each be seen in Figure 3. Exothermic peak 1 was relatively low; thus, exothermic peak 1 represents the low-temperature oxidation exotherm. As temperature increased, the chemical reaction rate and exothermic intensity both increased. When the reaction temperature reached exothermic peak 1, the amounts and types of reactive structures in the pulverized coal diminished because the structures were consumed by the long-run oxidation process. When the temperature increased to the stable structure cracking temperature, the structures cracked into minute molecular structures and commenced to participate in the oxidation reaction. The DSC curve of peak 2 exhibited an initially increasing trend. Thus, the initial temperature of exothermic peak 2 was defined as the ignition temperature (T_{ig}).[34]

3.2.2. Effects of Oxygen Concentrations on Ignition Temperatures. T_{ig} is the temperature at which the mechanism of the pulverized coal reaction abruptly transforms from oxidative dissociation to combustion.[34,39] The T_{ig} value of sample C was the highest, whereas that of sample B was the lowest (Table 3). The main reason for this result was that sample C was of a type known as high-metamorphic bituminous coal. The samples A and B were low and medium

metamorphic bituminous coals, respectively. The categories and quantities of the active structures of the samples A and B were adequate, and the two samples showed high oxidation activity and a low T_{ig}. With dwindling oxygen levels, T_{ig} increased. When compared with the T_{ig} value at an oxygen concentration of 21.0 vol. %, the T_{ig} value of sample A increased by 53.2 °C, sample B increased by 34.8 °C, and sample C increased by 58.0 °C at an oxygen concentration of 5.0 vol. %. As oxygen concentrations decreased, the reaction of the active structures with oxygen was inhibited. The low oxygen concentration restricted the number of types and amounts of intermediate active products and free radicals being generated. The free radicals were crucial in promoting the fracture of the stable chemical bonds of the pulverized coal. Therefore, the T_{ig} value of the pulverized coal samples augmented remarkably as the oxygen content abated.

3.2.3. Effects of Heating Rates on Ignition Temperatures. The ignition temperatures of the samples at various heating rates under the oxygen level of 21.0 vol. % are shown in Figure 4. Meanwhile, the relationship between ignition temperature
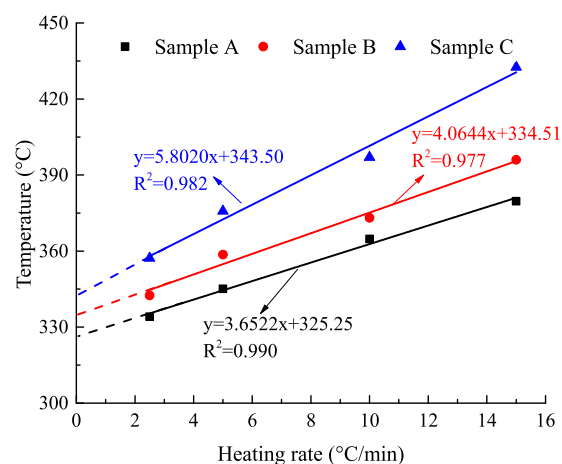
Figure 4. Ignition temperatures under various heating rates for an oxygen level of 21.0 vol. %.

and heating rate was linearly fitted. The slope indicated the increment of ignition temperature when the heating rate increased by 1 °C/min, and the intercept stands for the ignition temperature of pulverized coal under normal storage (no oxidation).

The T_{ig} value increased with an increase in the heating rate. The variation in the slopes of fitting curves indicated that the growth rate of T_{ig} for sample C was the highest, whereas for sample A, it was the lowest. For every 1.0 °C/min increase in the heating rate, the T_{ig} of sample C, B, and A increased by 5.80, 4.06, and 3.65 °C, correspondingly. The major cause for this situation was that the rose ramp rate shortened the oxidation time at specific temperatures, which curtailed the degree of oxidation and slowed the oxygen reaction.[40] In addition, the sample with high metamorphic grade contained
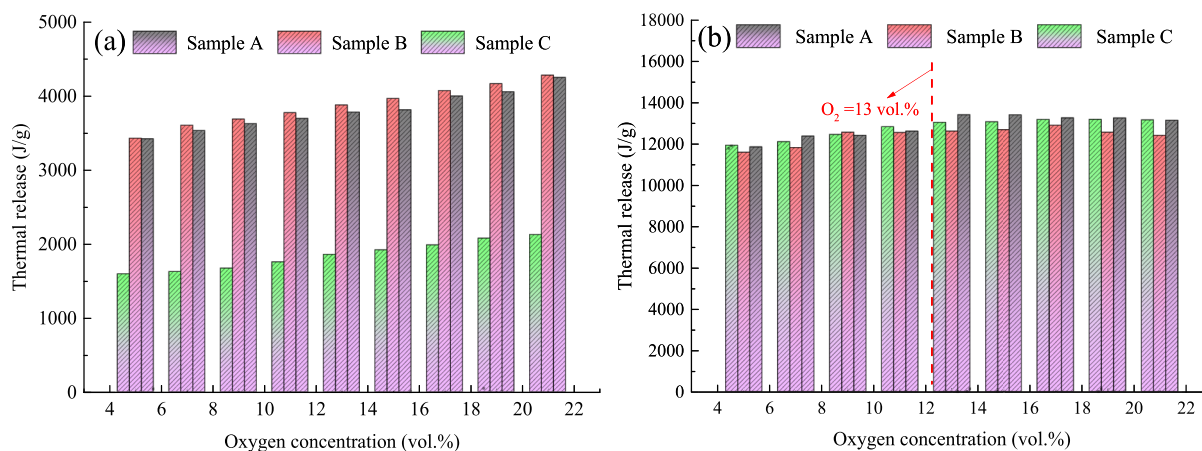
Figure 5. Thermal release of the three pulverized coal samples at different stages: (a) low-temperature oxidation stage and (b) combustion stage.
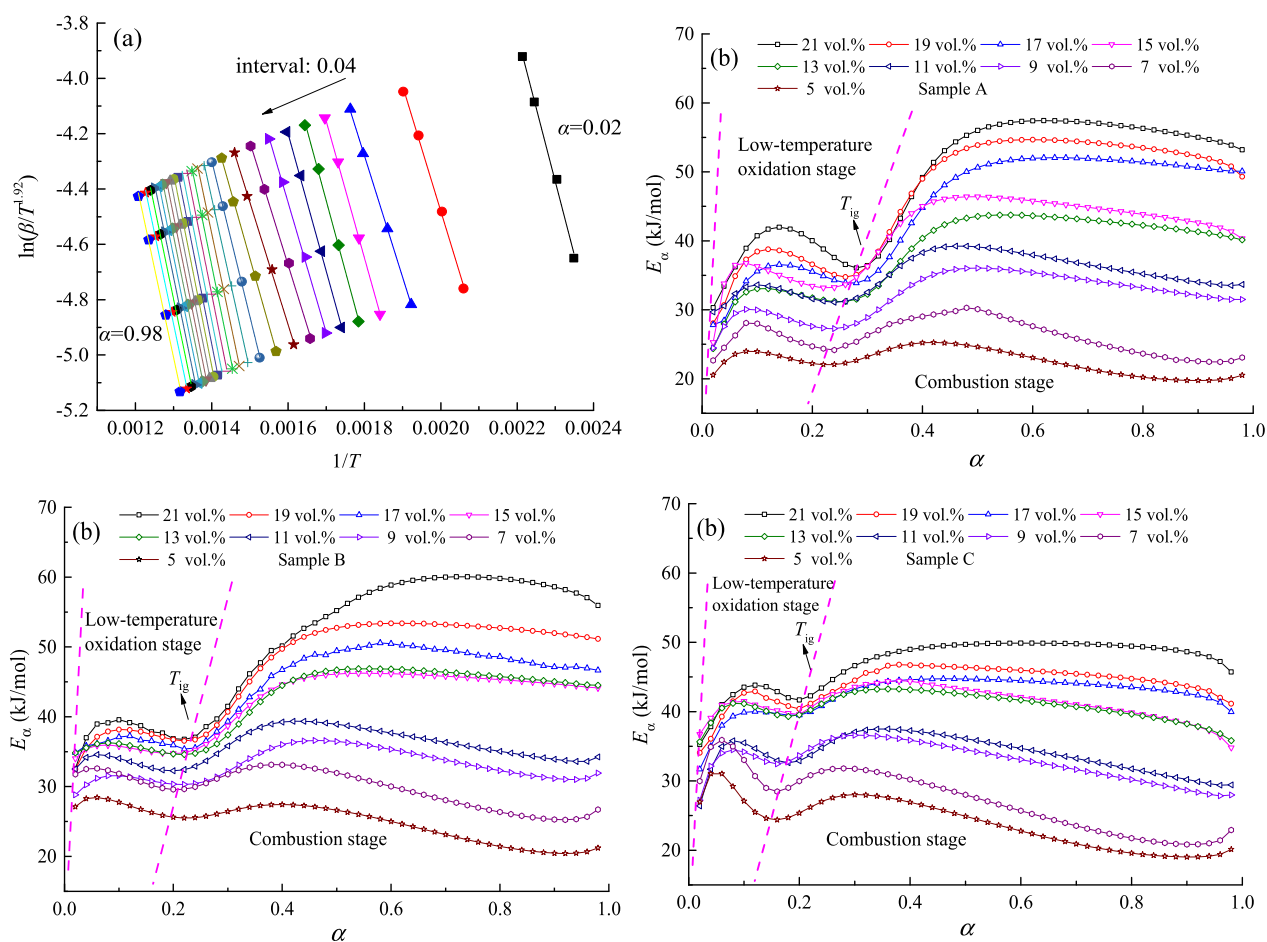

Figure 6. (a) Linear relationship between $\ln(\beta/T^{1.92})$ and $1/T$ and (b) apparent activation energies *vs* conversion degree of the pulverized coal samples.

more stable functional groups, which need more energy and longer time to initiate the reaction. Therefore, the sample with high metamorphic grade presented higher ignition temperature and more obvious influence by the heating rate.

3.3. Characteristics of Thermal Release at Different Stages. The oxidation combustion of the pulverized coal sample was divided into two reaction sections, a low-temperature oxidation stage and combustion stage, which were determined by the T_{ig} value. The thermal release data of

the pulverized coal at different stages and at a ramp rate of 5.0 °C/min are presented in Figure 5.

The thermal release at the low-temperature oxidation stage was saliently lower than that of the combustion stage (Figure 5). The types and amounts of activated structures were limited. Furthermore, a decrease in the oxygen concentration prominently inhibited low-temperature oxidative exothermic release. As the oxygen concentration attenuated, the thermal release levels within the low-temperature oxidation stage also decreased. Exothermic intensity also decreased during the

combustion stage. However, a low oxygen concentration did increase the reaction time (Figure 2). Therefore, at oxygen concentrations higher than 13.0 vol. %, the oxygen level had little effect on the exothermic reaction in the latter combustion stage. When the oxygen level was lower than 13.0 vol. %, the exothermic reaction in the combustion stage diminished (Figure 5b). The proposed reason for this phenomenon was that when the oxygen concentration was less than 13.0 vol. %, combustion was limited, which caused the exothermic strength to abridge remarkably. The low oxygen environment caused an increase in the amount of incompletely oxidized products that were produced by combustion; this inhibited the combustion exotherm of the test samples.

3.4. Apparent Activation Energy.
Taking the whole process of pulverized coal combustion as the object, the exotherm was obtained from the DSC curve integral. The conversion degree from 0.01 to 0.99 was picked up to analyze the thermodynamic parameter (apparent activation energy). In addition, the values of $\ln(\beta/T^{1.92})$ and $1/T$ were obtained for various conversion degrees (Figure 6a). The apparent activation energy at various atmospheres was computed using eq 4 (Figure 6b).

The apparent activation energy curves at various atmospheres were similar. Apparent activation energy exhibited an initially increasing trend, followed by a decreasing trend, with an increased conversion degree before T_{ig}. The conversion degree reached the minimum value near the ignition temperature. The apparent activation energy then showed an upward trend followed by a sharp decrease after the final maximum value was attained (Figure 6). The types of structures involved in the oxidation reaction increased with the rise in the reaction temperature, which also led to the apparent activation energy level to increase. The categories and quantities of active reactive chemical groups within the samples were limited, and the active structures were continuously consumed during oxidation. Therefore, as the amount of reactive structures decreased, the exothermic strength and apparent activation energy gradually decreased after their maximum values.[41] The amount of reactive structures substantially decreased because the duration of oxidation consumption increased and the activation temperature of the stable structures was not reached. Therefore, the apparent activation energy reached a minimum value near T_{ig}.[42]

After the temperature exceeded T_{ig}, numerous stable structures were activated and commenced to participate in the combustion.[43] Apparent activation energy increased with temperature. During combustion decay, apparent activation energy gradually decreased with an increase in temperature, then gradually decreased as the oxygen concentration decreased (Figure 6). The suggested reason for the aforementioned phenomena was that a reduction in the oxygen concentration resulted in a noticeable decline in the number of oxygen molecules that reacted with the pulverized coal. Moreover, a cutback in the oxygen concentration hindered the diffusion of oxygen molecules into the interior hole of the pulverized coal sample, resulting in a decrease in the types of structures (e.g., benzene ring, aromatic hydrocarbons, etc.) that required high-energy reactions, and the inhibition of the oxidative combustion reaction. Therefore, a particular oxygen concentration could be determined to effectively and substantially suppress the spontaneous combustion of pulverized coal.

3.5. Evaluation of the Risks of Spontaneous Combustion for Pulverized Coal.
To evaluate the risks of spontaneous combustion for pulverized coal at various oxygen concentrations, the ε values of the three pulverized coal samples were calculated according to eq 5. The calculated ε values of the samples at various oxygen-level atmospheres are shown in Figure 7.

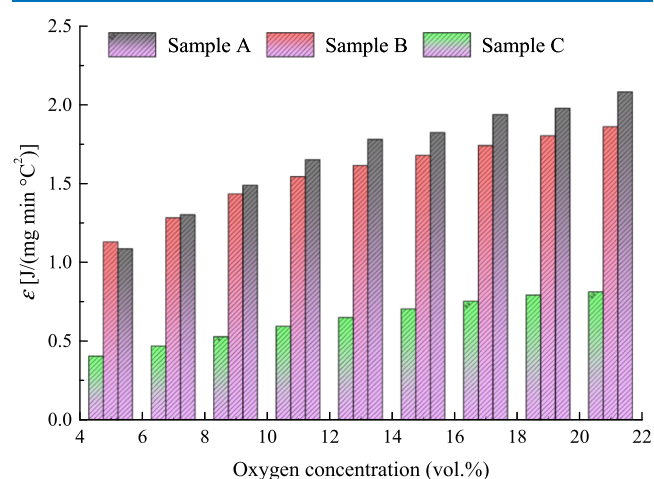**Figure 7.** ε values *vs* oxygen concentrations of the three pulverized coal samples at a heating rate of 5.0 °C/min.

The risks of spontaneous combustion index of sample C was less than that of the samples A and B. The reason for this phenomenon was the high metamorphic degree of sample C, due to which its oxidative exothermic ability significantly decreased (Figure 2). With a reduce in the oxygen level, the risk of spontaneous combustion for pulverized coal decreased (Lei et al. 2018). When the oxygen level was lowered from 21.0 to 5.0 vol. %, ε lessened from 2.07 (sample A), 1.85 (sample B), and 0.81 [J/(mg min °C²)] (sample C) to 1.08 (sample A), 1.13 (sample B), and 0.40 [J/(mg min °C²)] (sample C), respectively. A low oxygen level lessened the quantities of activated oxygen molecules and inhibited the diffusion of oxygen from the surface to the internal pores of the sample. Thus, reducing the oxygen concentration in the environment, where pulverized coal was stored, would be a simple, effective, and feasible method to greatly diminish or even prevent spontaneous combustion.

4. CONCLUSIONS

For further understanding the process of pulverized coal spontaneous combustion, this paper investigated the exothermic properties of pulverized coal under atmospheres with different oxygen concentrations. The related thermodynamic analysis was then carried out. The main findings are summarized as follows:

The exothermic process of pulverized coal during spontaneous combustion could be divided into two concentrated exothermic stages. With the decrease in the oxygen concentration, the exothermic rate under the same conversion decreased, and the concentrated exothermic process tended to be scattered, indicating that the exothermic process was suppressed. Meanwhile, a method to determine the ignition temperature based on peak fitting was proposed, and it was found that the ignition temperature increased with the increase

in the heating rate whereas decreased with the increase in the oxygen concentration.

The quantity of heat release at the combustion stage was much higher than that at low-temperature oxidation stage, and the quantity of heat release both at the two stages decreased with the decrease in the oxygen concentrations. Meanwhile, there was a critical value at which reducing the oxygen concentration would obviously inhibit the exothermic behaviors of pulverized coal. For the samples in this paper, the critical oxygen concentration was 13 vol. %.

The variation in apparent activation energy in the process of pulverized coal spontaneous combustion presented the "M" style and reached the minimum when the temperature was approximately ignition temperature. Taking the ignition temperature as the boundary, the apparent activation energy tended to first increase and then decrease when the temperature was below or above the ignition temperature. Weakened oxygen supply limits the probability of low-activity functional groups participating in the reaction, causing the decrease in apparent activation energy. Comprehensive analysis showed that reducing oxygen concentration could effectively suppress the risk of pulverized coal spontaneous combustion.

■ AUTHOR INFORMATION

Corresponding Authors

Lifeng Ren − *Xi'an University of Science and Technology, Xi'an 710054 Shaanxi, PR China; Post-doctoral Research Center of Mining Engineering, Xi'an University of Science and Technology, Xi'an 710054 Shaanxi, PR China;* orcid.org/0000-0001-9684-2218; Email: lifengrr@126.com

Qingwei Li − *Xi'an University of Science and Technology, Xi'an 710054 Shaanxi, PR China; Post-doctoral Research Center of Mining Engineering and School of Safety Science and Engineering, Xi'an University of Science and Technology, Xi'an 710054 Shaanxi, PR China;* Email: liqingwei90@126.com

Authors

Jun Deng − *Xi'an University of Science and Technology, Xi'an 710054 Shaanxi, PR China; School of Safety Science and Engineering, Xi'an University of Science and Technology, Xi'an 710054 Shaanxi, PR China; Shaanxi Key Laboratory of Prevention and Control of Coal Fire, Xi'an 710054 Shaanxi, PR China*

Li Ma − *Xi'an University of Science and Technology, Xi'an 710054 Shaanxi, PR China; School of Safety Science and Engineering, Xi'an University of Science and Technology, Xi'an 710054 Shaanxi, PR China*

Yang Xiao − *Xi'an University of Science and Technology, Xi'an 710054 Shaanxi, PR China; School of Safety Science and Engineering, Xi'an University of Science and Technology, Xi'an 710054 Shaanxi, PR China; Shaanxi Key Laboratory of Prevention and Control of Coal Fire, Xi'an 710054 Shaanxi, PR China;* orcid.org/0000-0002-3960-9708

Xiaowei Zhai − *Xi'an University of Science and Technology, Xi'an 710054 Shaanxi, PR China; School of Safety Science and Engineering, Xi'an University of Science and Technology, Xi'an 710054 Shaanxi, PR China; Shaanxi Key Laboratory of Prevention and Control of Coal Fire, Xi'an 710054 Shaanxi, PR China*

Jianchi Hao − *Xi'an University of Science and Technology, Xi'an 710054 Shaanxi, PR China; School of Safety Science and Engineering, Xi'an University of Science and Technology, Xi'an 710054 Shaanxi, PR China*

Complete contact information is available at:
https://pubs.acs.org/10.1021/acsomega.1c03160

Notes

The authors declare no competing financial interest.

■ REFERENCES

(1) Deng, J.; Yang, Y.; Zhang, Y.-N.; Liu, B.; Shu, C.-M. Inhibiting effects of three commercial inhibitors in spontaneous coal combustion. *Energy* **2018**, *160*, 1174−1185.

(2) Li, Q.-W.; Xiao, Y.; Zhong, K.-Q.; Shu, C.-M.; Lü, H.-F.; Deng, J.; Wu, S. Overview of commonly used materials for coal spontaneous combustion prevention. *Fuel* **2020**, *275*, 117981.

(3) Belošević, S.; Tomanović, I. D.; Beljanski, V.; Tucaković, D.; Živanović, T. Numerical prediction of processes for clean and efficient combustion of pulverized coal in power plants. *Appl. Therm. Eng.* **2015**, *74*, 102−110.

(4) Liu, Y.; Fu, P.; Zhang, B.; Yue, F.; Zhou, H.; Zheng, C. Study on the surface active reactivity of coal char conversion in O_2/CO_2 and O_2/N_2 atmospheres. *Fuel* **2016**, *181*, 1244−1256.

(5) Yang, F.; Qiu, D. Exploring coal spontaneous combustion by bibliometric analysis. *Process Saf. Environ. Protect.* **2019**, *132*, 1−10.

(6) Chen, Z.; Wang, Q.; Wang, B.; Zeng, L.; Che, M.; Zhang, X.; Li, Z. Anthracite combustion characteristics and NO x formation of a 300 MW e down-fired boiler with swirl burners at different loads after the implementation of a new combustion system. *Appl. Energy* **2017**, *189*, 133−141.

(7) Niu, Y.; Yan, B.; Liu, S.; Liang, Y.; Dong, N.; Hui, S. Ultra-fine particulate matters (PMs) formation during air and oxy-coal combustion: Kinetics study. *Appl. Energy* **2018**, *218*, 46−53.

(8) Yin, C.; Yan, J. Oxy-fuel combustion of pulverized fuels: combustion fundamentals and modelling. *Appl. Energy* **2016**, *162*, 742−762.

(9) Ouyang, Z.; Zhu, J.; Lu, Q.; Yao, Y.; Liu, J. The effect of limestone on SO_2 and NO_x emissions of pulverized coal combustion preheated by circulating fluidized bed. *Fuel* **2014**, *120*, 116−121.

(10) Chen, X.; Li, H.; Wang, Q.; Zhang, Y. Experimental investigation on the macroscopic characteristic parameters of coal spontaneous combustion under adiabatic oxidation conditions with a mini combustion furnace. *Combust. Sci. Technol.* **2018**, *190*, 1075−1095.

(11) Li, B.; Liu, G.; Bi, M. S.; Li, Z. B.; Han, B.; Shu, C. M. Self-ignition risk classification for coal dust layers of three coal types on a hot surface. *Energy* **2021**, *216*, 119197.

(12) Deng, J.; Liu, L.; Lei, C.; Wang, C.; Xiao, Y. Spatiotemporal distributions of the temperature and index gases during the dynamic evolution of coal spontaneous combustion. *Combust. Sci. Technol.* **2021**, *193*, 1679−1695.

(13) Xiao, Y.; Ren, S.-J.; Deng, J.; Shu, C.-M. Comparative analysis of thermokinetic behavior and gaseous products between first and second coal spontaneous combustion. *Fuel* **2018**, *227*, 325−333.

(14) Kuang, M.; Yang, G.; Zhu, Q.; Ti, S.; Wang, Z. Effect of burner location on flow-field deflection and asymmetric combustion in a 600 MWe supercritical down-fired boiler. *Appl. Energy* **2017**, *206*, 1393−1405.

(15) Li, Q.-W.; Xiao, Y.; Wang, C.-P.; Deng, J.; Shu, C.-M. Thermokinetic characteristics of coal spontaneous combustion based on thermogravimetric analysis. *Fuel* **2019**, *250*, 235−244.

(16) Jones, J. C. Recent developments and improvements in test methods for propensity towards spontaneous heating. *Fire Mater.* 1999, 23, 239−243.

(17) Pérez-Jeldres, R.; Cornejo, P.; Flores, M.; Gordon, A.; García, X. A modeling approach to co-firing biomass/coal blends in pulverized coal utility boilers: synergistic effects and emissions profiles. *Energy* 2017, 120, 663−674.

(18) Chen, Y.; Mori, S.; Pan, W.-P. Studying the mechanism of ignition of coal particles by TG-DTA. *Thermochim. Acta* 1996, 275, 149−158.

(19) Huang, X.; Jiang, X.; Han, X.; Wang, H. Combustion characteristics of fine and micro-pulverized coal in the mixture of O_2/CO_2. *Energy Fuel.* 2008, 22, 3756−3762.

(20) Yi, B.; Zhang, L.; Mao, Z.; Huang, F.; Zheng, C. Effect of the particle size on combustion characteristics of pulverized coal in an O_2/CO_2 atmosphere. *Fuel Process. Technol.* 2014, 128, 17−27.

(21) Yu, D.; Xu, M.; Sui, J.; Liu, X.; Yu, Y.; Cao, Q. Effect of coal particle size on the proximate composition and combustion properties. *Thermochim. Acta* 2005, 439, 103−109.

(22) Shen, J.; Liu, J.; Zhang, H.; Jiang, X. NO_x emission characteristics of superfine pulverized anthracite coal in air-staged combustion. *Energy Convers. Manag.* 2013, 74, 454−461.

(23) Sung, Y.; Moon, C.; Eom, S.; Choi, G.; Kim, D. Coal-particle size effects on no reduction and burnout characteristics with air-staged combustion in a pulverized coal-fired furnace. *Fuel* 2016, 182, 558−567.

(24) Deng, J.; Li, Q.; Xiao, Y.; Wen, H. The effect of oxygen concentration on the non-isothermal combustion of coal. *Thermochim. Acta* 2017, 653, 106−115.

(25) Deng, J.; Ren, L.-F.; Ma, L.; Lei, C.-K.; Wei, G.-M.; Wang, W.-F. Effect of oxygen concentration on low-temperature exothermic oxidation of pulverized coal. *Thermochim. Acta* 2018, 667, 102−110.

(26) Ren, L.-F.; Deng, J.; Li, Q.-W.; Ma, L.; Zou, L.; Laiwang, B.; Shu, C.-M. Low-temperature exothermic oxidation characteristics and spontaneous combustion risk of coal. *Fuel* 2019, 252, 238−245.

(27) Xiao, Y.; Li, Q.-W.; Deng, J.; Shu, C.-M.; Wang, W. Experimental study on the corresponding relationship between the index gases and critical temperature for coal spontaneous combustion. *J. Therm. Anal. Calorim.* 2017, 127, 1009−1017.

(28) Perdochova, M.; Derychova, K.; Veznikova, H.; Bernatik, A.; Pitt, M. The influence of oxygen concentration on the composition of gaseous products occurring during the self-heating of coal and wood sawdust. *Process Saf. Environ. Protect.* 2015, 94, 463−470.

(29) Qi, X.; Li, Q.; Zhang, H.; Xin, H. Thermodynamic characteristics of coal reaction under low oxygen concentration conditions. *J. Energy Inst.* 2017, 90, 544−555.

(30) Li, H.; Chen, X.; Shu, C.-M.; Wang, Q.; Ma, T.; Laiwang, B. Effects of oxygen concentration on the macroscopic characteristic indexes of high-temperature oxidation of coal. *J. Energy Inst.* 2019, 92, 554−566.

(31) Deng, J.; Ren, L.-F.; Ma, L.; Qin, X.-Y.; Wang, W.-F.; Liu, C.-C. Low-temperature oxidation and reactivity of coal in O_2/N_2 and O_2/CO_2 atmospheres, a case of carboniferous-permian coal in Shaanxi, China. *J. Environ. Earth Sci.* 2019, 78, 234.

(32) Fu-bao, Z.; Bo-bo, S.; Jian-wei, C.; Ling-jun, M. A New approach to control a serious mine fire with using liquid nitrogen as extinguishing media. *Fire Technol.* 2013, 51, 325−334.

(33) Vyazovkin, S.; Burnham, A. K.; Criado, J. M.; Pérez-Maqueda, L. A.; Popescu, C.; Sbirrazzuoli, N. ICTAC Kinetics Committee recommendations for performing kinetic computations on thermal analysis data. *Thermochim. Acta* 2011, 520, 1−19.

(34) Zhang, Y.; Liu, Y.; Shi, X.; Yang, C.; Wang, W.; Li, Y. Risk evaluation of coal spontaneous combustion on the basis of auto-ignition temperature. *Fuel* 2018, 233, 68−76.

(35) Chao, J.; Yang, H.; Wu, Y.; Zhang, H.; Lv, J.; Dong, W.; Xiao, N.; Zhang, K.; Xu, C. The investigation of the coal ignition temperature and ignition characteristics in an oxygen-enriched FBR. *Fuel* 2016, 183, 351−358.

(36) Liu, B.; Zhang, Z.; Zhang, H.; Yang, H.; Zhang, D. An experimental investigation on the effect of convection on the ignition behaviour of single coal particles under various O_2 concentrations. *Fuel* 2014, 116, 77−83.

(37) Niu, S. L.; Lu, C. M.; Han, K. H.; Zhao, J. L. Thermogravimetric analysis of combustion characteristics and kinetic parameters of pulverized coals in oxy-fuel atmosphere. *J. Therm. Anal. Calorim.* 2009, 98, 267−274.

(38) Deng, J.; Li, B.; Xiao, Y.; Ma, L.; Wang, C.-P.; Lai-wang, B.; Shu, C.-M. Combustion properties of coal gangue using thermogravimetry-Fourier transform infrared spectroscopy. *Appl. Therm. Eng.* 2017, 116, 244−252.

(39) Ávila, I.; Crnkovic, P. M.; Luna, C. M. R.; Milioli, F. E. Use of a fluidized bed combustor and thermogravimetric analyzer for the study of coal ignition temperature. *Appl. Therm. Eng.* 2017, 114, 984−992.

(40) Deng, J.; Wang, K.; Zhang, Y.; Yang, H. Study on the kinetics and reactivity at the ignition temperature of Jurassic coal in north Shaanxi. *J. Therm. Anal. Calorim.* 2014, 118, 417−423.

(41) Ren, L.-F.; Li, Q.-W.; Deng, J.; Yang, X.; Ma, L.; Wang, W.-F. Inhibiting effect of CO_2 on the oxidative combustion thermodynamics of coal. *RSC Adv.* 2019, 9, 41126−41134.

(42) Xiao, Y.; Lü, H.-F.; Huang, A.-C.; Deng, J.; Shu, C.-M. A new numerical method to predict the growth temperature of spontaneous combustion of 1/3 coking coal. *Appl. Therm. Eng.* 2018, 131, 221−229.

(43) Yi, X.; Xiao, Y.; Lü, H.-F.; Shu, C.-M.; Deng, J. Thermokinetic behavior and microcharacterization during the spontaneous combustion of 1/3 coking coal. *Combust. Sci. Technol.* 2018, 191, 1769−1788.